Electronic properties of C_{60}/InP(001) heterostructures

Electronic properties of C_{60}/InP(001) heterostructures

G Cherkashinin[1,2,3]**, S Krischok**[1,2]**, M Himmerlich**[1,2]**, O Ambacher**[2] **and J A Schaefer**[1,2]

[1] Institute of Physics, Technical University Ilmenau, D-98684 Ilmenau, Germany
[2] Institute of Micro- and Nanotechnologies, Technical University Ilmenau, D-98684 Ilmenau, Germany

E-mail: gennady.cherkashinin@staff.hu-berlin.de

Abstract
The growth of fullerene films on the InP(001)-(2×4) surface and the formation of the C_{60}/InP(001)-(2×4) interface were studied by x-ray photoelectron spectroscopy, ultraviolet photoelectron spectroscopy, electron energy loss spectroscopy and low energy electron diffraction. C_{60} adsorption causes weak ($\sim$0.15 eV) upward band bending at the interface. Thick C_{60} films form an fcc (111) structure on the InP(001) surface. The (2×4) reconstruction is preserved beneath the C_{60} film. The photoelectron measurements yield a valence band discontinuity of 0.88 ± 0.20 eV at the C_{60}/InP(001)-(2×4) interface.

1. Introduction

Indium phosphide plays an important role for microelectronic applications. It is used as a material in microwave power devices and as an active layer in optoelectonics. The unique property of C_{60} on InP(001) is that thick C_{60} films form ordered layers on InP(001) in an fcc (111) structure [1, 2]. Therefore, the knowledge of the interface properties of the semiconductor heterostructure is of great interest. The electronic properties of a semiconductor heterostructure are determined by the band structure alignment across the interface. The band discontinuities of heterojunctions are key design parameters, since the valence and conduction band offsets, ΔE_V and ΔE_C, determine the transport and confinement properties at the interface.

The interaction of C_{60} with InP(001)-(2×4) has been studied by a number of surface sensitive techniques [1–3]. The growth mechanism of C_{60} molecules on InP(001) as well as the bonding at the interface were studied by scanning tunnelling microscopy (STM), (high resolution) electron energy loss spectroscopy ((HR)EELS), x-ray and ultraviolet photoelectron spectroscopy (XPS, UPS) and low energy electron diffraction (LEED) [1, 2]. Nevertheless, publications devoted to the study of the electronic properties of the C_{60}/InP(001) interface

---

[3] Present address: Institute of Physical and Theoretical Chemistry, Humboldt-University Berlin, Brook-Taylor-Straße 2, D-12489 Berlin, Germany.

are rather rare. To our knowledge, information about the valence band discontinuity at the C_{60}/InP(001) interface is not available. In this paper a study of the electronic properties of the C_{60}/InP(001) heterostructure investigated by photoelectron spectroscopy in combination with LEED is reported.

2. Experimental details

For our investigations we used undoped InP(001) substrates from MCP Wafer Technology, Ltd with an intrinsic n-type carrier concentration lower than 10^{16} cm^{-3}. After loading the sample into an ultrahigh vacuum (UHV) chamber (base pressure below 10^{-10} Torr), the following cleaning procedure was used. First, the sample was annealed at 373 K for 24 h; this was followed by successive cycles of ion sputtering with Ar$^+$ ($E = 0.5$ keV, $I = 1$ μA) and annealing at 573 K until no impurities could be detected by XPS and a sharp InP(100)-(2 × 4) surface reconstruction was observed by LEED. The sample temperature was controlled with a K-type thermocouple.

$\qquad$ C_{60} was evaporated from a properly cleaned quartz cell onto the well-ordered InP(001)-(2 × 4) surface at room temperature. During C_{60} deposition the chamber pressure was about 2×10^{-10} Torr. Photoemission spectra were acquired using a hemispherical analyser (Leybold LH). The photoelectron spectra were recorded at normal emission. The analyser setting used leads to an energy resolution of 1.0 eV for the photoelectron spectra measured with an Al Kα source ($h\nu = 1486.6$ eV) and 0.15 eV for the spectra measured using He I ($h\nu = 21.2$ eV) and He II ($h\nu = 40.8$ eV) radiation. In all cases the Fermi level of the analyser was adjusted to the vacuum level, E_{vac}, of the sample by an internal bias. In this case, the work function of the sample can be directly determined from the low kinetic energy secondary electron cutoff of the spectra. An additional external bias of -5 V was applied to the sample during the secondary electron cutoff measurements in order to distinguish between analyser and sample cutoff. All binding energies are referred to the Fermi level of an Au plate. The thickness of the C_{60} films was calculated from the C1s/In3d$_{5/2}$ photoemission intensity ratio assuming a layer-by-layer growth model. Annealing of the C_{60}/InP(001) heterostructure was performed in four cycles between 543 and 573 K. We did not heat the C_{60}/InP(001) heterostructure at higher temperatures, as the In metallic clusters are formed on the InP(001) surface above 620 K [4]. Semiconductor properties of the InP(001) surface were also controlled by EELS. No surface or bulk plasmon peaks related to metallic indium were observed.

3. Results and discussion

3.1. C_{60}/InP(001) interface formation

The C_{60}/InP(001) interface formation was investigated using LEED in combination with photoelectron spectroscopy. The atom arrangement at the surface/interface is directly related to the electronic structure, therefore any changes in the surface reconstruction of the InP(001) lead to changes in the shape of the photoelectron spectra related to the semiconductor support.

$\qquad$ Figure 1 shows the evolution of the LEED pattern as a function of the C_{60} coverage. A sharp (2 × 4) surface reconstruction of the clean InP(001) has been observed in the LEED pattern measured at a primary beam energy of $E_0 = 72$ eV, figure 1(a). The corresponding XPS spectra of the InP(001)-(2 × 4) surface are in agreement with previous studies. For instance, the measured binding energies of the bulk and surface states of InP match well to the literature data [3, 5–7]. The In4d spectrum of the InP(001)-(2 × 4) surface obtained by UPS (He II) together with a decomposition of this core level into one bulk and two surface components is presented in figures 2(a) and (b) for various C_{60} coverages.
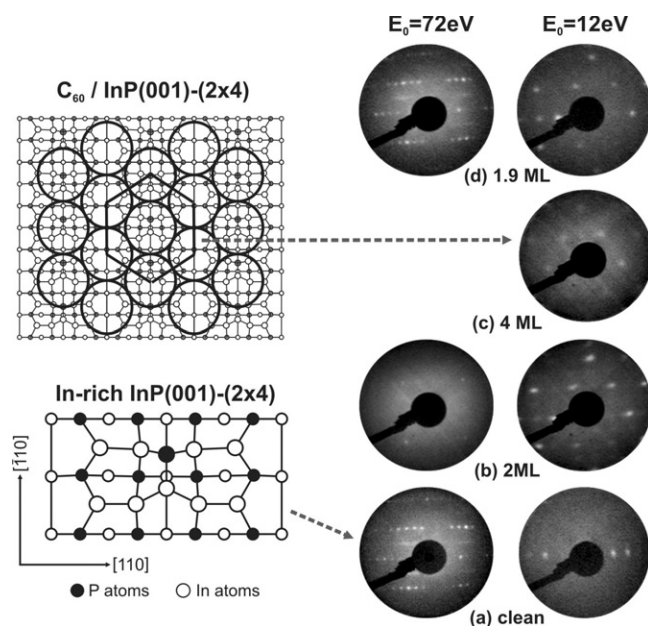
Figure 1. LEED images measured at the normal incidence geometry with 72 and 12 eV electron beam energy, respectively: (a) clean InP(001)-(2 × 4); (b), (c) 2 and 4 ML of the C$_{60}$ film, respectively; (d) 1.9 ML of C$_{60}$ (after fourth cycle of annealing of the C$_{60}$/InP(001) at 573 ± 20 K). On the left: unit cell of InP(001)-(2 × 4) (bottom) [19] and the hexagonal structure of the fcc (111) surface formed after adsorption of C$_{60}$ (top) [2]; the molecular unit cell is shown by the hexagon.

After deposition of 2 ML C$_{60}$, spots characteristic for both C$_{60}$ and InP are visible in the LEED pattern at $E_0 = 12$ eV (figure 1(b)). This observation indicates the formation of ordered C$_{60}$ crystals of at least a few hundreds of angstroms size, since the typical LEED coherence length is ∼100 Å [8]. After deposition of 2 ML of C$_{60}$, the In4d photoelectron spectrum (figures 2(a), (b)) shows a shift of 0.15 eV towards the Fermi level (E_F). We attribute this to a small upward band bending or, in other words, a small charge delocalization of substrate electrons over the C$_{60}$ molecule which has been reported for many C$_{60}$/metal interfaces [9, 10]. However, the shape of the In4d spectrum does not change compared to clean InP(001), including the spectral signature (In–P and In–In surface components) which is typical for the (2 × 4) reconstructed surface. This implies that the (2 × 4) surface reconstruction is not influenced by the fullerene adsorption.

At 4 ML C$_{60}$ coverage, the hexagonal structure, originating from the fcc (111) plane of C$_{60}$, is well resolved and no contribution from the substrate is observed in the diffraction pattern, see figure 1(c). The complete disappearance of the substrate spots suggests that a continuous film covers the substrate. The In4d photoelectron spectrum excited by He II radiation vanishes at this coverage, figure 2(a), as the electron's inelastic mean free path (IMFP) is a few angstroms at a kinetic energy $E_k \sim 20$ eV [13].

The annealing of the C$_{60}$/InP(001) heterostructure at 543–573 K results in the desorption of C$_{60}$ from the InP surface. However, the molecules do not desorb completely at these temperatures; sharp spots characteristic for C$_{60}$ occur in the LEED patterns. The weak chemical interaction of C$_{60}$ with the InP surface bonds provides enhanced surface mobility of the molecules even at moderate temperatures (543–573 K) and promotes the formation of a well-ordered structure of the film. In the case of strong chemical interaction, like for
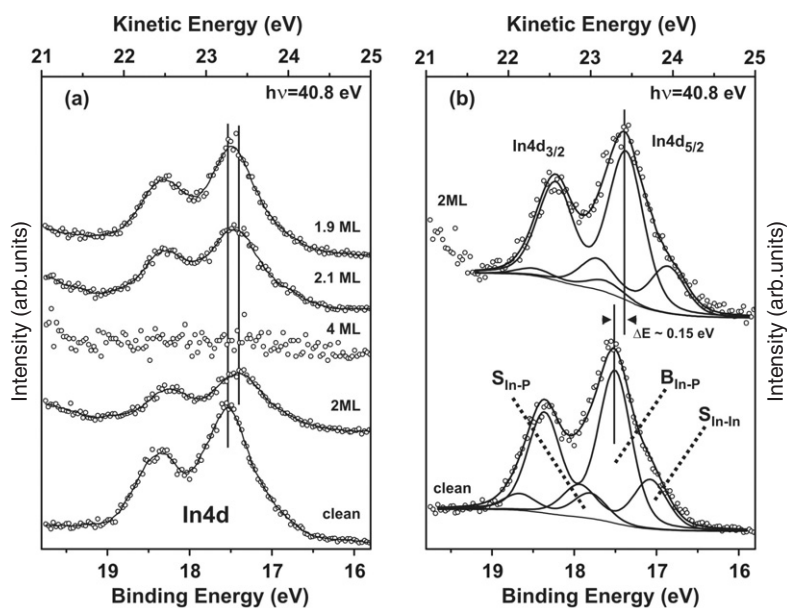
Figure 2. (a) The evolution of the In4d core level as a function of C_{60} coverage followed by annealing. The In4d core level (2.1 ML) was measured after the first cycle of the annealing at $T = 543 \pm 20$ K. (b) Decomposition of the In4d core-level spectrum with the three doublets taking into account spin–orbital splitting and a Shirley background [3, 11, 12]. For convenience, the peak measured at 2 ML of C_{60} coverage (b) is rescaled to the same height as the clean InP(001) (a). The spin–orbital splitting and branching ratio were kept fixed for the fitting (0.86 and 0.65 eV, respectively). The B_{In-P} component is attributed to the bulk In–P bond; the S_{In-In} surface component relates to the In surface bonding site which is characterized by a relative charge accumulation with respect to the phosphorous-coordinated bulk indium and exhibits a core-level shift compared to the bulk component by 0.30 ± 0.02 eV [3, 5–7]; the S_{In-P} surface component is due to the charge transfer from indium to phosphorous surface atoms and exhibits a core-level shift compared to the bulk component by -0.40 ± 0.03 eV.

C_{60}/Si(100), the ordering of the fullerene–semiconductor film cannot be reached even at the enhanced temperatures due to the low mobility of the C_{60} over the template [8]. After the fourth annealing cycle of the C_{60}/InP(001) heterostructure, the initial LEED pattern, characteristic for the InP(001)-(2 × 4) surface, reappears at $E_0 = 72$ eV, although the C_{60} phase is still detected at $E_0 = 12$ eV (see figure 1(d)). The fact that the solid fullerene phase bound by weak van der Waals intermolecular forces is more easily desorbed compared to the thin C_{60} film indicates weak chemisorption rather than physisorption of the fullerene at the InP(001) surface. This is in agreement with previous works demonstrating that C_{60} weakly chemisorbs on the InP(001) surface [3]. Desorption of the fullerene from the substrate results in a shift of the photoelectron core-level spectra towards their initial energetic position without visible changes in the shape of the spectra, figure 2(a).

Thus, the joint analysis of the electronic properties and the structure of the C_{60}/InP(001) interface indicate that the (2 × 4) reconstruction is preserved beneath the C_{60} film.

3.2. Electronic properties of the C_{60}/InP(001) heterostructure

Figure 3(b) shows the valence band spectrum of clean InP(001)-(2 × 4). The structures below the Fermi level labelled as B_I and B_{II} correspond to bulk states [14–18], while S_I
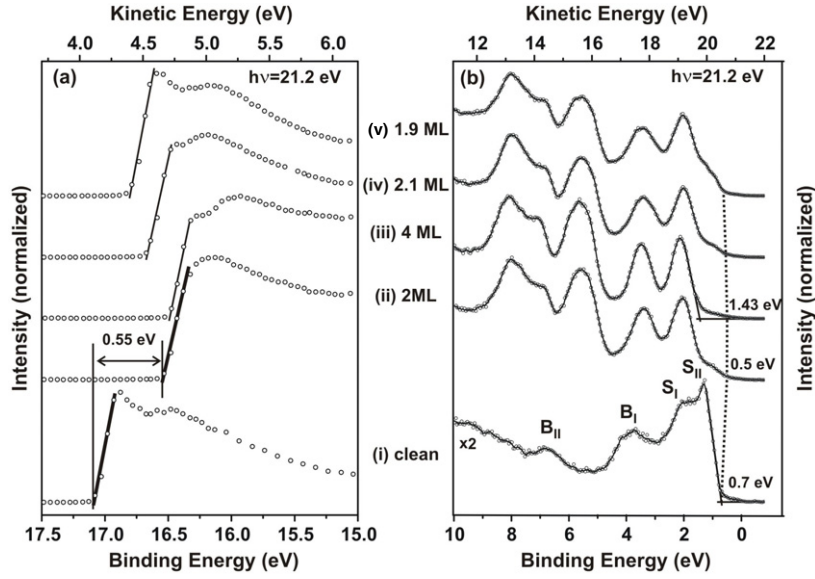
Figure 3. (a) The evolution of the high binding energy side of the He I excited photoelectron spectra via C$_{60}$ deposition (i), (ii), (iii) followed by annealing of the C$_{60}$/InP(001) heterostructure at $T = 543 \pm 20$ K (iv) and 573 ± 20 K (v). All spectra are shown after subtracting the sample bias of -5 V from the kinetic energy scale. The work function is determined by linear extrapolation of the secondary electron cutoff. It increases from about 4.15 up to 4.70 eV upon adsorption of 2 ML of the C$_{60}$ film. (b) The evolution of the valence band structure via the C$_{60}$ deposition followed by annealing of the C$_{60}$/InP(001) heterostructure. The valence band maximum, E_{VBM}, is determined by linear extrapolation of the valence band edge to the baseline. The dotted line shows the evolution of the $E_{\text{VBM}}^{\text{InP}}$ upon C$_{60}$ adsorption.

and S$_{\text{II}}$ are due to emission from the surface states of InP(001)-(2 × 4) [19]. According to first principle calculations, S$_{\text{I}}$ relates to the strongly localized mixed dimer bonds [19], while S$_{\text{II}}$ includes four surface states [19, 20] which cannot be resolved by the conventional photoelectron spectroscopy techniques. Both the S$_{\text{I}}$ and the S$_{\text{II}}$ features are very sensitive to adsorbed species and disappear rapidly after exposure to gases [21]. The onset energy $E_{\text{F}} - E_{\text{VBM}}^{\text{InP}}$ of the valence band emission can be determined from the well-known energy differences reported earlier on the InP(100) bulk electronic structure: $E_{\text{VBM}}^{\text{InP}} - E(\text{S}_{\text{II}}) = 0.6$ eV, $E_{\text{VBM}}^{\text{InP}} - E(\text{B}_{\text{II}}) = 6.0$ eV and $E_{\text{VBM}}^{\text{InP}} - E(\text{In4d}_{5/2}) = 16.9$ eV [14]. From our experimental data $[E_{\text{F}} - E(\text{S}_{\text{II}})]_{\text{exp}} = 1.30 \pm 0.05$ eV, $[E_{\text{F}} - E(\text{B}_{\text{II}})]_{\text{exp}} = 6.75 \pm 0.05$ eV, $[E_{\text{F}} - E(\text{In4d}_{5/2})]_{\text{exp}} = 17.50 \pm 0.05$ eV together with the above-mentioned energy differences, we determine an onset energy of $E_{\text{F}} - E_{\text{VBM}}^{\text{InP}} = 0.70 \pm 0.10$ eV. This value is close to the photoemission results reported earlier for InP(001) [22, 23]. The same valence band maximum, $E_{\text{VBM}}^{\text{InP}}$, is found by the linear interpolation of the onset of the valence band emission to the baseline, as illustrated in figure 3(b). From the secondary electron cutoff, figure 3(a), the work function was determined to $e\phi = 4.15 \pm 0.10$ eV. The obtained value is in a good agreement with previous results for the clean InP(001) surface [24]. The ionization potential, I_{p}, is determined as the distance between the valence band maximum and the vacuum level, E_{vac}, which leads to $I_{\text{p}}^{\text{InP}} = 4.85 \pm 0.10$ eV for InP. The fundamental band gap of InP is $E_{\text{g}}^{\text{InP}} = 1.34$ eV [25]. Therefore, the electron affinity is calculated to be $\chi = I_{\text{p}}^{\text{InP}} - E_{\text{g}}^{\text{InP}} = 3.51 \pm 0.10$ eV.

C$_{60}$ adsorption causes an $E_{\text{VBM}}^{\text{InP}}$ shift of 0.20 ± 0.10 eV towards E_{F} as illustrated in figure 3(b). As the shift in the same direction is observed for the core-level photoelectron

peaks related to the InP substrate (not shown here), we assign it to the upward band bending by 0.15 eV that is due to the formation of the C_{60}/InP(001) interface. With increasing C_{60} coverage, the observed E_{VBM}^{InP} shifts towards the Fermi level and decreases in intensity, indicating that the signal stems from the InP and is not related to the adsorbed fullerenes, see figure 3. Upon annealing, its intensity increases, indicating a particular desorption of C_{60}. The spectrum recorded from a 4 ML thick C_{60} film on InP(001)-(2 × 4) shows the typical electronic features of bulk C_{60}: HOMO (2.2 eV), HOMO-1 (3.5 eV), σ_s (5.7 eV) and σ_p (8.2 eV) [27]. By linear extrapolation of the high kinetic energy tail of the HOMO derived structure we obtain the valence band maximum E_{VBM}^{C60} of the C_{60} film at 1.43 ± 0.05 eV below the Fermi level. Considering this value and the binding energy $E_F - E(C1s) = 284.60 \pm 0.10$ eV we determine the binding energy $E_{VBM}^{C60} - E(C1s)$ of the C 1s core level with respect to the valence band maximum as 283.20 ± 0.10 eV. This agrees with data reported for solid fcc-C_{60} [28]. Adsorption of C_{60} modifies the sample work function $e\phi$. A change in work function can be a result of two contributions: (i) an adsorbate-induced band bending change, $e\Delta V_s$, and (ii) an interface dipole layer, $e\Delta\phi_{dip}$ [27] which results in an overall change of $e\Delta\phi = e\Delta V_s + e\Delta\phi_{dip}$. Changes of the surface dipole are present when the work function of a sample changes without changing the Fermi level position relative to the energy bands. If the shift of the Fermi level and the work function are of the same magnitude there is no change of the surface dipole. Figure 3(a) demonstrates that the work function increases by ~0.55 eV ($e\phi = 4.70 \pm 0.10$ eV) for 2 ML C_{60} film thickness. Since the adsorbate-induced upward band bending is only ~0.15 eV, the work function shift is evidently explained by changes in the surface dipole ($e\Delta\phi_{dip} = 0.40 \pm 0.10$ eV) rather than by a shift of E_F. Our data result in an ionization potential equal to $I_p^{C60} = 6.16 \pm 0.10$ eV for C_{60}.

The electronic properties of the C_{60}/InP(001)-(2 × 4) heterostructure are determined by the band structure alignment across the interface. The valence band discontinuity, ΔE_{VBM}, between C_{60} and InP is determined from the difference in the valence band maxima for the clean InP(001) and bulk C_{60} taking into account the upward band bending deduced from the XPS and UPS (He II) core-level measurements. We conclude a valence band discontinuity between 4 ML C_{60} and InP of $\Delta E_{VBM} = 0.88 \pm 0.20$ eV. Figure 4 displays schematically the band diagram of C_{60}/InP(001)-(2 × 4) heterostructure. The valence band discontinuity can be expressed in terms of the conduction band discontinuity, ΔE_C, since $\Delta E_{VBM} + \Delta E_C = \Delta E_g$ [30], where ΔE_g is the difference in the band gaps of two materials. However, neither the value nor the sign of ΔE_C can be reliably determined from the obtained experimental value of the valence band discontinuity. This is due to the larger scatter of the band gap energy reported for solid C_{60} which ranges from 1.3 eV up to 2.3 eV [27, 31–33]. To estimate the conduction band offset, we assume a band gap energy of $E_g^{C60} = 1.80 \pm 0.50$ eV [33]. By using the band gaps of InP and C_{60}, the conduction band offset is $\Delta E_C = -0.42 \pm 0.70$ eV, as indicated in figure 4. The electron affinity of the thick C_{60} film has been found to be $\chi = I_p^{C60} - E_g^{C60} = 4.36 \pm 0.60$ eV.

4. Conclusions

In the present work, we have studied the formation of the C_{60}/InP(001)-(2 × 4) interface and the alignment of the electronic band structure at this interface. For the deposition of the C_{60} molecules no essential charge transfer between C_{60} and the InP(001)-(2 × 4) surface has been found that could point to an ionic bonding at the interface. The C_{60} grows in fcc structure with (111) surface orientation and the InP(001)-(2 × 4) reconstruction is preserved beneath the C_{60} film. The C_{60} absorption causes weak upward band bending (~0.15 eV) and induces an interface dipole of $e\Delta\phi_{dip} = 0.40 \pm 0.10$ eV. The valence band discontinuity is determined to be $\Delta E_{VBM} = 0.88 \pm 0.20$ eV.
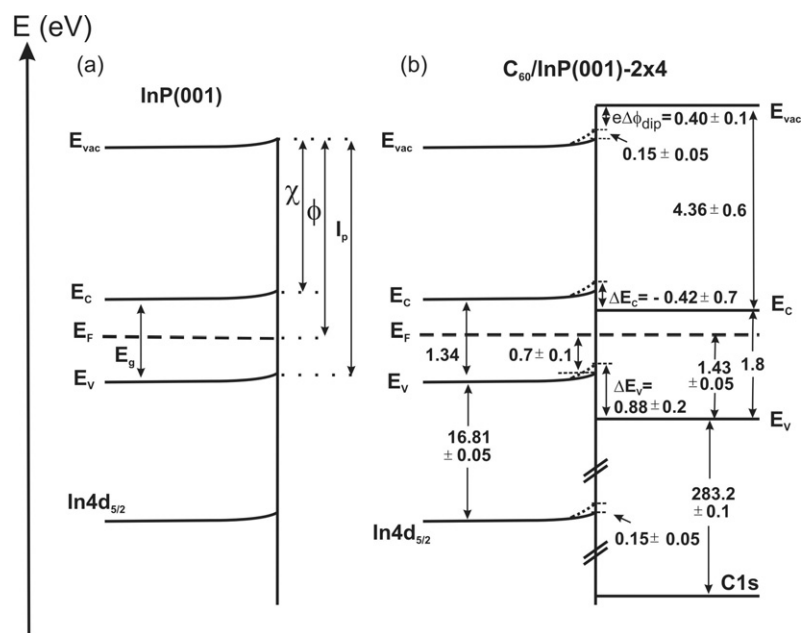
Figure 4. Energy band diagram of (a) the clean InP(001)-(2 × 4) and (b) the C_{60}/InP(001)-(2 × 4) interface. The band gap E_g, the work function $e\phi$ and the ionization potential I_p are shown. Although the studied InP(001) is undoped, intrinsic n-type carriers result in a shift of the Fermi level closer to the conduction band, E_C, than to the valence band E_V. Therefore, the upward band bending near the clean InP(001) surface is shown. The band bending induced by C_{60} adsorption is shown by the dotted lines. All numbers are given in eV.

The high mobility of the C_{60} molecules at the semiconductor substrate, at appropriate temperatures, implies that InP(001) can be a useful template for epitaxial growth of the fullerenes. In the present study we have gained information on the band structure at the interface, which is important for the design of new electronic devices based on this material system.

References

[1] Schaefer J A, Cherkashinin G, Döring S, Eremtchenko M, Krischok S, Malsch D, Opitz A and Stolz T 2004 Surface science tools and their application to nanosystems like C_{60} on indium phosphide *Frontiers of Multifunctional Integrated Nanosystems: Proc. NATO Advanced Research Workshop (Ilmenau, Germany, July 2003)* (*NATO Science Series, II-Mathematics, Physics and Chemistry* vol 64) ed E Buzaneva and P Scharff (Dordrecht: Kluwer Akademic Publishers) pp 131–8
[2] Eremtchenko M, Döring S, Temirov R and Schaefer J A 2005 *Phys. Rev.* B **71** 045410
[3] Chao Y, Svensson K, Radosavkic D, Dhanak V R, Siller L and Hunt M R C 2001 *Phys. Rev.* B **64** 235331
[4] Chao Y, Svensson K, Radosavkic D, Dhanak V R, Hunt M R C and Siller L 2002 *Phys. Rev.* B **66** 075323
[5] Kinsky J, Chultz Ch, Pahlke D, Frisch A M, Herrmann T, Esser N and Richter W 1998 *Appl. Surf. Sci.* **123** 228
[6] Chab V, Pekarek L, Ulrych I, Suchy J, Prince K C, Peloi M, Evans M, Comicioli C, Zacchigna M and Crotti C 1997 *Surf. Sci.* **377–379** 261
[7] Shimomura M, Sanada N, Kaneda G, Takeuchi T, Suzuki Y, Fukuda Y, Huff W R A, Abukawa T, Kono S, Yeom H W and Kakizaki A 1998 *Surf. Sci.* **412–413** 625
[8] Gensterblum G, Yu L-M, Pireaux J-J, Thiry P A, Caudano R, Themlin J-M, Bouzidi S, Coletti F and Debever J-M 1993 *Appl. Phys.* A **56** 175
[9] Ohno T R, Chen Y, Harvey S E, Kroll G H, Weaver J H, Haufler R E and Smalley R E 1991 *Phys. Rev.* B **44** 13747

[10] Maxwell A J, Brütwiler P A, Nilsson A, Martensson N and Rudolf P 1994 *Phys. Rev.* B **49** 10717

[11] Gebhardt R K, Sloboshanin S, Schaefer J A and Chasse T 1999 *Appl. Surf. Sci.* **142** 94

[12] Chao Y, Svensson K, Radosavkic D, Dhanak V R, Hunt M R C and Siller L 2002 *Phys. Rev.* B **66** 075323

[13] Seah M P and Dench W A 1979 *Surf. Interface Anal.* **1** 2

[14] Lodders F, Westhof J, Schaefer J A, Höpfinger H, Goldmann A and Witzel S 1991 *Z. Phys.* B **83** 263

[15] Chelikowsky J R and Cohen M L 1976 *Phys. Rev.* B **14** 556

[16] Ley L, Pollak R A, McFeely R F, Kowalczyk S P and Shirley D A 1974 *Phys. Rev.* B **9** 600

[17] Williams G P, Cerrina F, Lapeyre G J, Anderson J R and Hermanson J 1986 *Phys. Rev.* B **34** 5548

[18] Sorba L, Hinkel V, Middelmann H U and Horn K 1987 *Phys. Rev.* B **36** 8075

[19] Schmidt W G, Esser N, Frisch A M, Vogt P, Bernholc J, Bechstedt F, Zorn M, Hannappel Th, Visbeck S, Willig F and Richter W 2000 *Phys. Rev.* B **61** R16335

[20] Schmidt W G, Briggs E L, Bernholc J and Bechstedt F 1999 *Phys. Rev.* B **59** 2234

[21] Weiss W, Hornstein R, Schmeisser D and Göpel W 1990 *J. Vac. Sci. Technol.* B **8** 715

[22] Huff W R, Shimomura M, Sanada N, Kaneda G, Takeuchi T, Suzuki Y, Yeom H W, Abukawa T, Kono S and Fukuda Y 1998 *Phys. Rev.* B **57** 10132

[23] Moison J M and Bensoussan M 1986 *Surf. Sci.* **168** 68

[24] Stietz F, Allinger Th, Polyakov V, Woll J, Goldmann A, Erfurth W, Lapeyre G J and Schaefer J A 1996 *Appl. Surf. Sci.* **104–105** 169

[25] Madelung O, Schulz M and Weis H (ed) 1982 *Semiconductors, Physics of II–VI and I–VII Compounds* (*Landolt-Börnstein New Series* vol 17) (Berlin: Springer)

[26] Lüth H 1993 *Surfaces and Interfaces of Solids* (Berlin: Springer)

[27] Weaver J H, Martins J L, Komeda T, Chen Y, Ohno T R, Kroll G H, Troullier N, Haufler R E and Smalley R E 1991 *Phys. Rev. Lett.* **66** 1741

[28] Janzen O and Moench W 1999 *J. Phys.: Condens. Matter* **11** L111

[29] Kraut E A, Grant R W, Waldrop J R and Kowalczyk S P 1980 *Phys. Rev. Lett.* **44** 1620

[30] Waldrop J R and Grant R W 1979 *Phys. Rev. Lett.* **43** 1686

[31] Zhou W, Xie S, Qian S, Wang G and Qian L 1996 *J. Phys.: Condens. Matter* **8** 5793

[32] Lof R W, van Veenendaal M A, Koopmans B, Jonkman H T and Sawatzky G A 1992 *Phys. Rev. Lett.* **68** 3924

[33] Hansen P L, Fallon P J and Krätschmer W 1991 *Chem. Phys. Lett.* **181** 367